Available online at www.sciencedirect.com
ScienceDirect
Optical Materials 30 (2007) 184–187
OPTICAL Materials
www.elsevier.com/locate/optmat

Structural and optical properties of Nd- and Tb-doped BaY_2F_8

Mário E.G. Valerio [a,*], Viviane G. Ribeiro [a], Ana C.S. de Mello [a], Marcos A.C. dos Santos [a], Sonia L. Baldochi [b], Vera L. Mazzocchi [b], Carlos B.R. Parente [b], Robert A. Jackson [c,1], Jomar B. Amaral [a]

[a] *Physics Department, Federal University of Sergipe, 49, 100-000 São Cristovão, SE, Brazil*
[b] *IPEN-CNEN/SP, CP 11049, 05422-970, São Paulo, SP, Brazil*
[c] *School of Physical and Geographical Sciences, Keele University, Keele, Staffs ST5 5BG, UK*

Available online 12 January 2007

Abstract

In the present work, we report the optical properties of rare-earth doped BaY_2F_8 and its potential use as a scintillator in radiation detection. The samples were synthesized and grown by the zone melting method under a HF flow. X-ray powder diffraction was performed and quantitative phase analysis was done using the Rietveld method. Emission and excitation spectra of the doped samples were measured at room temperature. The identification of the transitions was done comparing the excitation and emission peaks with the results obtained from computer modelling. The scintillator properties of the pure and doped samples were checked by measuring the radioluminescence of the sample when excited with different types of radiation, revealing that these materials are promising radiation detectors.
© 2006 Elsevier B.V. All rights reserved.

PACS: 78.55.−m; 78.60.Ya; 78.20.Bh

Keywords: BaY_2F_8; Rare-earth doping; Scintillator; PL spectra; Computer modelling

1. Introduction

Mixed metal fluorides, when doped with rare-earth ions (RE), are promising materials for solid-state optical devices, mainly when one of the metal ions of the matrix is Y. BaY_2F_8 (BYF) has recently been used in a number of applications, involving, respectively, doping by Er [1], Pr [2], Tm [3] and Dy [4]. In addition, a new modelling strategy for predicting optical transitions of RE^{3+} ions has been devised recently and applied to the BYF matrix [5].

In the present work Nd- and Tb-doped BYF samples were prepared and studied via XRD powder diffraction, photoluminescence (PL) and radioluminescence (RL). XRD allowed the structural characterisation of the produced samples as well as the determination of the amount of incorporation of the RE^{3+} ions in the BYF matrix. PL measurements allowed the identification of the main optical active transitions of the RE dopant and the RL measurements proved that RE-doped BYF is a promising material for scintillating detectors. Computer modelling helped the identification of all radiative transitions observed in the PL and RL spectra.

2. Methodology

The synthesis of RE-doped BYF was performed in a platinum reactor from stoichiometric mixture of BaF_2 and YF_3. Nd, Er and Tb were added in concentrations from 2–3 mol%. The starting materials were melted at 960 °C under a HF flow in Pt crucibles. The crystals were prepared from the synthesized powders by the zone melting

* Corresponding author. Tel.: +55 79 32173558; fax: +55 79 3212 6807.
E-mail addresses: mvalerio@fisica.ufs.br (M.E.G. Valerio), r.a.jackson@chem.keele.ac.uk (R.A. Jackson).
[1] Fax: +44 1782 712378.

0925-3467/$ - see front matter © 2006 Elsevier B.V. All rights reserved.
doi:10.1016/j.optmat.2006.11.037

method, under HF atmosphere. Powder samples were prepared by grinding the obtained materials in a mortar.

XRD measurements were performed at room temperature in a Rigaku DMAX 2000/PC diffractometer. The powder XRD patterns were taken in the 2θ range from 12 to 80° in step scan mode, with steps of 0.02°, using Cu Kα radiation. Quantitative phase analysis was done using the Rietveld method. Additional to the determination of the phase concentrations, lattice parameters, fractional atomic coordinates, site-occupancies and anisotropic thermal parameters were refined in the analyses.

PL excitation and emission spectra were recorded at room temperature for the single crystals in an ISS PC1 spectrofluorimeter using a 300 W Xe lamp source, with excitation and emission wavelength resolution of 4.0 and 2.0 nm, respectively.

RL spectra were recorded exciting the samples with Cu Kα radiation. The spectra were collected using an optical fibre conducting the light to an Ocean Optics HR2000 spectrometer.

The computer modelling strategy employed here followed the procedure described in [5], which is summarised as follows: (i) The incorporation of M^{3+} dopants into the BYF structure was carried out using the Mott–Littleton method [6,7] employed in the GULP code [8]; (ii) crystal field parameters (B^k_q) were calculated for the lowest energy configuration, using the theory of Judd [9] and Ofelt [10], and the simple overlap model (SOM) [11,12]; (iii) The energy levels were computed using the SPECTRA code [16], with the calculated B^k_q parameters and free ion parameters (ζ, α, β, γ, T^i, M^i and P^i) from [13]. All possible mechanisms of incorporation of the RE^{3+} were considered and the full set of B^k_qs was determined for all RE^{3+} ions. In the present work the procedure was repeated for Tb^{3+} and these energy levels were used to help the identification of the main optical transitions observed in the BYF:Tb^{3+} samples. In [5] it was found that the lowest solution energy was obtained for all M^{3+} dopants at the Y^{3+} site, and this has been assumed in the rest of this paper.

3. Results and discussions

XRD powder patterns were measured for all samples and the sample composition, lattice parameters and site-occupancies were obtained by Rietveld analysis. Fig. 1 shows the experimental and refined patterns of the synthesized and single crystals of BYF:Tb^{3+}. It can be seen that, although other undesirable crystalline phases (YF_3 and $Ba_4Y_3F_{17}$) were found in the synthesized sample, in the zone melted single crystals none of them were present. Also, it is seen that the amount of dopant actually dissolved is about 3 mol% for both dopants (see Table 1). The lattice parameters obtained for both doped samples are consistent with expected behaviour given that the ionic radius of Nd^{3+} is about 10% higher than for Y^{3+} [14]. The lattice slightly expanded after Nd^{3+} incorporation and the final cell volume was 312.2 Å^3, as compared to the 308.8 Å^3

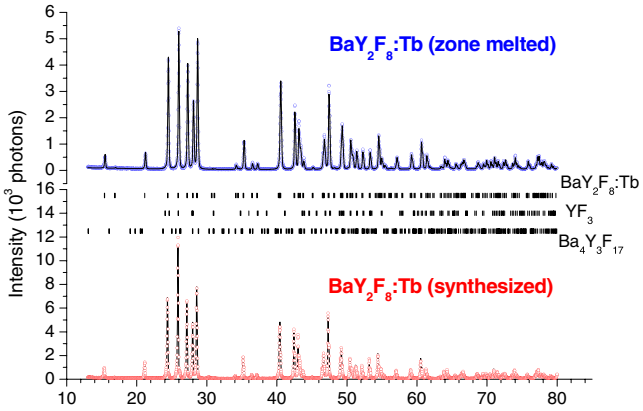


Fig. 1. XRD powder pattern of the synthesized samples and single crystals of BYF:Tb^{3+}. Continuous lines indicate the refined pattern.

Table 1
Composition of the synthesized samples and single crystals obtained from the Rietveld refinement of the XRD data

Sample	Crystalline phases	Lattice parameters (Å)	Composition	Calculated lattice parameters (Å)
Synthesised				
Nd:BYF	BaY_2F_8:Nd		80.88 mol%	
	YF_3		14.88 mol%	
	$Ba_4Y_3F_{17}$		4.24 mol%	
Tb:BYF	BaY_2F_8:Tb		93.86 mol%	
	YF_3		5.61 mol%	
	$Ba_4Y_3F_{17}$		0.53 mol%	
Single crystals				
Nd:BYF	BaY_2F_8:Nd	$a = 6.977$	Occupancy:	$a = 6.984$
		$b = 10.508$	Y:0.96748	$b = 10.740$
		$c = 4.259$	Nd:0.03252	$c = 4.214$
		$\beta = 99.7°$		$\beta = 98.3°$
Tb:BYF	BaY_2F_8:Tb	$a = 6.971$	Occupancy:	$a = 6.976$
		$b = 10.499$	Y:0.97126	$b = 10.731$
		$c = 4.256$	Tb:0.02874	$c = 4.209$
		$\beta = 99.7°$		$\beta = 98.2°$

Calculated lattice parameters were also quoted and were obtained using the *Y* site occupancy as determined from the XRD.

for pure BYF [15]. However, the Tb^{3+} ion is only slightly larger than Y^{3+} ($r_{Tb^{3+}} = 0.923$ Å and $r_{Y^{3+}} = 0.9$ Å, both have six-fold coordination [14]) and the lattice slightly expanded to 311.5 Å^3. The modelling strategy reproduced these trends quite well giving volumes of 311.8 Å^3 and 312.8 Å^3 for the Tb^{3+} and Nd^{3+} doped systems.

The scintillator properties of RE^{3+}-doped BYF are shown in Fig. 2. This shows the RL spectra of the Tb^{3+}-doped samples excited by X-rays as compared to the PL measurements excited with UV light at 368 nm. The emission spectra are equivalent indicating that the Tb^{3+} ion is the emission centre responsible for the scintillating process. It is worth noting that when exciting with X-ray and ion beams this sample displays a very intense green light.

PL excitation and emission spectra of the Tb^{3+}-doped BYF were converted to wavenumbers and all transitions

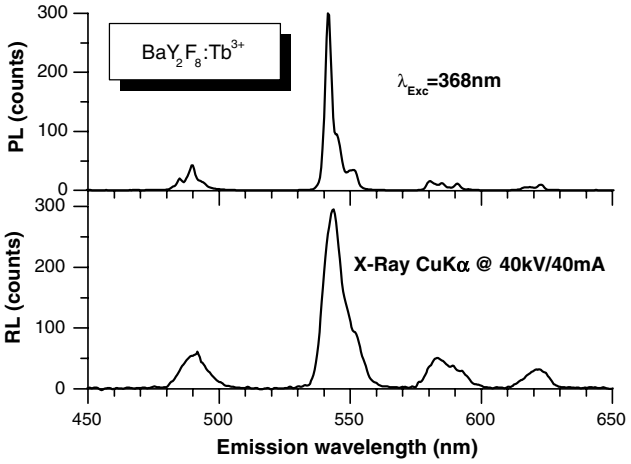


Fig. 2. RL and PL spectra of the BYF:Tb^{3+} single crystals.

were deconvoluted in the spectra and an example of that is shown in Fig. 3 for the main emission centred at 18 500 cm^{-1}.

The energy levels obtained by the computer modelling strategy are shown in Table 2. Not all levels were included in the table but just the ones important to identify the RL and the PL emission and excitation spectra.

Comparing the excitation spectra with the energy levels it is possible to conclude that the maximum at 374 nm (26 773 cm^{-1}) is due to the excitation from the $^7F_6$ ground level to the $^5D_3$ levels, while the excitation at 368 nm (27.174 cm^{-1}) corresponds to the $^5L_{10}$, $^5G_6$ and $^5H_6$ related levels. The excitation at 350 nm (28 571 cm^{-1}) is due to the $^5G_5$ and $^5H_5$ related levels and the excitation at 257 nm (38 910 cm^{-1}) is clearly due to the $^5H_5 + {}^5I_5$.

On the other hand, most of the emission lines observed either in the PL and the RL spectra are not due to transitions to the ground state of the Tb^{3+} ions. The most intense emission in the 17 700–18 800 cm^{-1}, as an example, is due to the transition of the $^5D_4 \rightarrow {}^7F_4$ and $^5D_4 \rightarrow {}^7F_5$. The experimental values of the upper and lower wavenumbers for $^5D_4 \rightarrow {}^7F_4$ transitions are 17 181 and 18 037 cm^{-1}, while

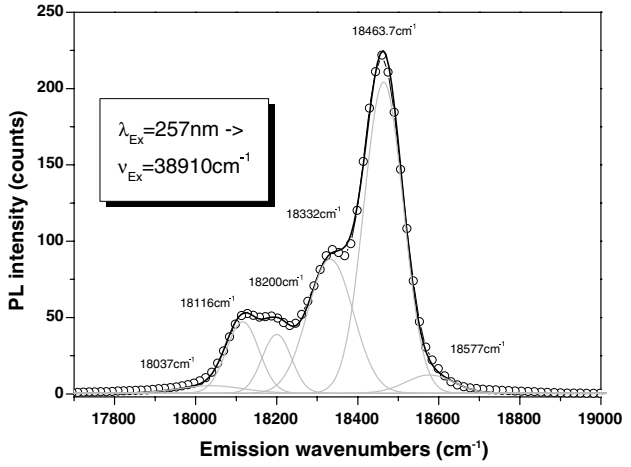


Fig. 3. Deconvolution of the PL spectra of the BYF:Tb^{3+} single crystals in the 18 400 cm^{-1} spectral region.

Table 2
Calculated energy levels for Tb^{3+} in BYF, assuming substitution at the Y^{3+} site

Energy (cm^{-1})	Term symbol
0, 5, 13, 24, 75, 105, 107, 108, 114, 189, 193, 215, 216	$^7F_6$
2203, 2214, 2230, 2235, 2254, 2279, 2303, 2311, 2339, 2405, 2407	$^7F_5$
3526, 3548, 3584, 3590, 3624, 3640, 3651, 3723, 3794	$^7F_4$
4511, 4544, 4577, 4586, 4596, 4604, 4607	$^7F_3$
5146, 5153, 5227, 5266	$^7F_2$
5306	$^7F_2 + {}^5D_2$
5582, 5613, 5660	$^7F_1 + {}^5D_1$
5812	$^7F_0 + {}^5D_0$
21 518, 21 521, 21 528, 21 533, 21 534, 21 536, 21 538, 21 567	$^5D_4$
26 927, 26 928, 26 929, 26 932, 26 933, 26 941, 26 955	$^5D_3$
27 235, 27 242, 27 254	$^5L_{10} + {}^5G_6$
27 262, 27 266	$^5L_{10}$
27 282, 27 295, 27 306, 27 310, 27 320, 27 327, 37 374, 27 382, 27 399	$^5L_{10} + {}^5G_6$
27 402, 27 410	$^5L_{10} + {}^5G_6 + {}^5H_6$
27 413	$^5L_{10} + {}^5G_6$
27 431, 27 433	$^5G_6$
27 460, 27 464	$^5L_{10}$
27 470, 27 473, 27534.3, 27534.4	$^5L_{10} + {}^5G_6$
28 362, 28 364, 28 377, 28 389, 28 408, 28 412	$^5G_5 + {}^5H_5$
28 414	$^5G_5$
28 422	$^5G_5 + {}^5H_5$
28 429	$^5G_5$
28 460, 28 464	$^5G_5 + {}^5H_5$
28 627.4, 28627.7, 28 633, 28633.4, 28 666, 28 672, 28 675, 28 683, 28 686, 28 701, 28 708, 28 719, 28 725, 28 816, 28 819, 28 820, 28 822, 28 890, 28 890	$^5L_9$
28 946, 28 952, 28 958, 28 961, 28 965	$^5D_2 + {}^3P_2$
–	–
39 293, 39 297, 39 297, 39 302, 39 321, 39 322, 39 341, 39 353, 39 381, 39 383, 39 387	$^5H_5 + {}^5I_5$

the calculated wavenumbers are 17 724 and 18 041 cm^{-1}, a difference as lower as 3%. For the $^5D_4 \rightarrow {}^7F_5$ transitions the experimental values are 18 116 and 19 900 cm^{-1} and the calculated ones are 19 111 and 19 364 cm^{-1}, and the percentage differences are within 3–5%.

All the other transitions shown in the RL and PL emission spectra could be identified in this way and the average difference is about 3%, representing an excellent agreement and showing that the predictions of the modelling strategy are helpful in interpreting the emission spectra of the RE^{3+} ions embedded in the crystalline matrix.

4. Conclusions

This work demonstrated that BYF doped with RE^{3+} ions are promising solid-state systems for radiation detection and possible applications of single crystals of BYF:RE^{3+} may be devised in scintillators due to their high output light yield and also the useful wavelength emission that can be tuned by choosing the RE^{3+} dopant that matches the light detection device. It was also shown that

the modelling strategy that includes a combination of defect calculation, crystal field evaluation and 4f energy level splitting is very useful in helping the clear identification of the transitions of the RE^{3+} dopant. In particular, for Tb^{3+} in the BYF matrix, an overall agreement around 3% was attained between the experimental and calculated photon energies due to the 4f–4f transitions.

Acknowledgement

The authors are grateful to MCT/PADCTIII, FINEP, CNPq and CAPES for financial support and MSc grants.

References

[1] E. Sani, A. Toncelli, M. Tonelli, Optics Express 13 (2005) 8984.
[2] A. Richter, N. Pavel, E. Heumann, G. Huber, D. Parisi, A. Toncelli, M. Tonelli, A. Diening, W. Seelert, Optics Express 14 (2006) 328.
[3] N. Coluccelli, G. Galzerano, P. Laporta, D. Parisi, A. Toncelli, M. Tonelli, Optics Express 14 (2006) 1518.
[4] D. Parisi, A. Toncelli, M. Tonelli, E. Cavalli, E. Bovero, A. Belletti, J. Phys.: Condens. Matter 17 (2005) 2783.
[5] J.B. Amaral, M.A. Couto dos Santos, M.E.G. Valerio, R.A. Jackson, Appl. Phys. B (2005) 841.
[6] N.F. Mott, M.J. Littleton, Trans. Faraday Soc. 34 (1938) 485.
[7] C.R.A. Catlow, J. Chem. Soc. Faraday Trans. II 85 (1989) 335.
[8] J.D. Gale, J. Chem. Soc. Faraday Trans. 93 (1997) 629.
[9] B.R. Judd, Phys. Rev. 127 (1962) 750.
[10] G.S. Ofelt, J. Chem. Phys. 37 (1962) 511.
[11] O.L. Malta, Chem. Phys. Lett. 88 (1982) 353.
[12] P. Porcher, M.A. Couto dos Santos, O.L. Malta, Phys. Chem. Chem. Phys. 1 (1999) 397.
[13] W.T. Carnall, G.L. Goodman, K. Rajnak, R.S. Rana, J. Chem. Phys. 90 (1989) 3443.
[14] R.D. Shannon, Acta Cryst. A 32 (1976) 751.
[15] N. Magnani, G. Amoretti, A. Baraldi, R. Capelletti, Radiat. Eff. Defect. Sol. 157 (2002) 921.
[16] G.K. Liu, <http://chemistry.lanl.gov/downloads/spectra>.